



## Second malignant neoplasm risk after craniospinal irradiation in X-ray-based techniques compared to proton therapy

Vasanthan Sakthivel<sup>1,2</sup> · Kadirampatti M. Ganesh<sup>2,3</sup> · Craig McKenzie<sup>4,5</sup> · Raghavendiran Boopathy<sup>1</sup> · Jothybasu Selvaraj<sup>6,7</sup> 

Received: 11 July 2018 / Accepted: 24 January 2019 / Published online: 6 February 2019  
© Australasian College of Physical Scientists and Engineers in Medicine 2019

### Abstract

Cranio-spinal irradiation (CSI) is widely used for treating medulloblastoma cases in children. Radiation-induced second malignancy is of grave concern; especially in children due to their long-life expectancy and higher radiosensitivity of tissues at young age. Several techniques can be employed for CSI including 3DCRT, IMRT, VMAT and tomotherapy. However, these techniques are associated with higher risk of second malignancy due to the physical characteristics of photon irradiation which deliver moderately higher doses to normal tissues. On the other hand, proton beam therapy delivers substantially lesser dose to normal tissues due to the sharp dose fall off beyond Bragg peak compared to photon therapy. The aim of this work is to quantify the relative decrease in the risk with proton therapy compared to other photon treatments for CSI. Ten anonymized patient DICOM datasets treated previously were selected for this study. 3DCRT, IMRT, VMAT, tomotherapy and proton therapy with pencil beam scanning (PBS) plans were generated. The prescription dose was 36 Gy in 20 fractions. PBS was chosen due to substantially lesser neutron dose compared to passive scattering. The age of the patients ranged from 3 to 12 with a median age of eight with six male and four female patients. Commonly used linear and a mechanistic doseresponse models (DRM) were used for the analyses. Dose-volume histograms (DVH) were calculated for critical structures to calculate organ equivalent doses (OED) to obtain excess absolute risk (EAR), life-time attributable risk (LAR) and other risk relevant parameters. A  $\alpha'$  value of  $0.018 \text{ Gy}^{-1}$  and a repopulation factor  $R$  of 0.93 was used in the mechanistic model for carcinoma induction. Gender specific correction factor of 0.17 and  $-0.17$  for females and males were used for the EAR calculation. The relative integral dose of all critical structures averaged were 6.3, 4.8, 4.5 and 4.7 times higher in 3DCRT, IMRT, VMAT and tomotherapy respectively compared to proton therapy. The mean relative LAR calculated from the mean EAR of all organs with linear DRM were 4.0, 2.9, 2.9, 2.7 higher for male and 4.0, 2.9, 2.8 and 2.7 times higher for female patients compared to proton therapy. The same values with the mechanistic model were 2.2, 3.6, 3.2, 3.8 and 2.2, 3.5, 3.2, 3.8 times higher compared to proton therapy for male and female patients respectively. All critical structures except lungs and kidneys considered in this study had a substantially lower OED in proton plans. Risk of radiation-induced second malignancy in Proton PBS compared to conventional photon treatments were up to three and four times lesser for male and female patients respectively with the linear DRM. Using the mechanistic DRM these were up to two and three times lesser in proton plans for male and female patients respectively.

**Keywords** Second malignancy · Proton therapy · Craniospinal irradiation · EAR · LAR · Childhood malignancy · VMAT · IMRT · Tomotherapy

✉ Jothybasu Selvaraj  
Jothy.Selvaraj@act.gov.au

<sup>1</sup> Advanced Medical Physics, Houston, USA

<sup>2</sup> Research and Development Centre, Bharathiar University, Coimbatore, India

<sup>3</sup> Department of Radiation Physics, Kidwai Memorial Institute of Oncology, Bengaluru, India

<sup>4</sup> Department of Radiation Oncology, Miami Cancer Institute, Miami, USA

<sup>5</sup> RaySearch Laboratories, New York, USA

<sup>6</sup> Medical Physics & Radiation Engineering, Canberra Hospital, Garran, ACT, Australia

<sup>7</sup> South West Clinical School, University of New South Wales, Sydney, Australia

## Introduction

Tumors of the central nervous system (CNS) is the most common malignant brain tumor in children and a rare brain tumor in adults [1]. It starts in the cerebellum, which controls balance and other complex motor and cognitive functions. Medulloblastoma is also one of the most radiosensitive childhood brain tumors [2], therefore radiation therapy (RT) is justly considered to be the treatment standard of care. Radiotherapy for medulloblastoma entails irradiation of the entire cranio-spinal axis with a homogeneous dose, and hence termed cranio-spinal irradiation (CSI). Several X-ray-based techniques are employed for CSI including 3D conformal RT (3DCRT), intensity modulated RT (IMRT), volumetric modulated arc therapy (VMAT), and helical tomotherapy (HT). Recently proton beam therapy (PBT) has been proposed to reduce late effects. The pros and cons of each of these techniques are multifactorial, including dosimetric benefits, costs involved and complexity in planning and delivery.

Dosimetric benefits of these techniques have been widely studied in literature [3–6]. The major difference in terms of dose distribution between these techniques is that intensity modulated X-ray-based techniques have higher monitor units (MU) compared to 3DCRT and deliver relatively higher doses to healthy tissues compared to both 3DCRT and PBT. However, intensity modulated techniques are preferred due to their superior conformity of higher dose to, and homogeneity of dose within the target volume which results in better sparing of organs-at-risk (OAR) and higher tumor control. Though this is beneficial in the short-term, relatively higher doses delivered to healthy tissues is of grave concern in children, which is shown by atomic bomb survivors database, this concern is due to their higher genetic susceptibility and due to smaller body size in children compared to adults which results in a larger extent of body exposed to low dose levels through leakage and scattered radiation [7, 8]. The most recent childhood cancer survivor study (CCSS) showed long-term survivors of childhood cancer who received radiotherapy have a significantly increased risk of developing second malignant neoplasms (SMNs) [9]. In fact, IMRT has been shown to double the risk of SMNs compared to conventional techniques [10]. However, it's worth mentioning here that the 5-year survival rate for pediatric patients have increased from 30 to 80% since 1960 due to advancements in pediatric cancer care [11]. The 5-year survival rate for children with medulloblastoma is substantially higher (73%) [9]; while 30-year cumulative incidence of SMNs is also shown to be high (31%) [11]. It is not ideal for patients with such a high survival rate to have doubled the risk of SMN's posed by using IMRT.

According to the literature the key factor for reducing the SMNs is to improve the treatment regimens [12]. The major factor that is considered to be associated with SMNs after radiotherapy is the higher dose to healthy tissues. PBT offers superior OAR sparing whilst also delivering much lower doses to healthy tissues due to the characteristic Bragg peak observed in proton irradiation. PBT can be delivered either by passive scattering or an active scanning method, which is also known as pencil beam scanning. However, the passive scanning technique uses scattering foils to broaden the beam which becomes a source of neutrons that have a relative biological effectiveness (RBE) of 10 [13] and hence have proportionately higher risk of SMNs compared to IMRT. This fact supports the use of pencil beam scanning (PBS) method over passive scattering. It has been emphasized in the literature that the long-term risks of particle therapies will not be known for many years since these techniques have only gained momentum recently and availability of sufficient long-term clinical follow-ups are far from conclusive. Therefore, theoretical risk assessment techniques based on existing knowledge of SMNs have been proposed in the literature to quantify the risk of these techniques [14] and justify the use of protons over X-ray-based radiotherapy. Several studies have evaluated the risk of SMNs in current techniques and protons in various sites either using phantoms or patients' treatment plans [15–21]. However, comprehensive analyses of SMN risk in all or most of the techniques available to date using real patients' datasets in CSI is rare. Moreover, several dose–response models (DRM) for SMN have been proposed in the literature in addition to the commonly used linear-no-threshold (LNT) model [22]. Furthermore, male and female patients have been shown to have different SMN response to radiotherapy [9, 23–25]. This has been hypothesized due to the increased activity of cytochrome p450 enzyme and effects of estrogen in female patients [26].

The aim of this study is to quantify the risk of SMN in CSI for male and female pediatric patients using the LNT and a mechanistic DRM that takes cell proliferation and mutation into account in 3DCRT, IMRT, VMAT, HT and pencil beam scanning PBT.

## Materials and methods

### Patient selection and contouring

Ten pediatric patients approved by the institutional review board with a mean age of 8 years ranging between 3 and 12 years with six male and four female patients were available for this study. CT scans which were previously used for conventional (3DCRT) CSI planning and treatment were selected and anonymized. Treatment planning was performed in Monaco® treatment planning system (Elekta

Medical Systems, Stockholm) consistent with Sharma et al. [27]. The PTV of the brain and spine were generated by growing a uniform volumetric margin of 0.5 cm and 1 cm in all directions over the corresponding CTVs respectively.

## Treatment planning

Five separate treatment plans including 3DCRT, IMRT, VMAT, HT and a pencil beam scanning PBT plan were generated for each patient. Daily fractional dose of 1.8 Gy was delivered in 20 fractions according to the institutional planning protocol. 3DCRT, IMRT and VMAT plans were generated in the Monaco® planning system whereas HT were planned on Tomotherapy planning station (Tomotherapy Inc, Madison, WI) and pencil beam scanning PBT were planned on RayStation planning system (RaySearch Labs, Stockholm, Sweden). Monte Carlo based dose calculation engine was the preferred choice in Monaco for 3DCRT, IMRT and VMAT plans since it is more accurate in calculating doses at low levels (where SMN risk can be high) than other model-based algorithms. A variance (statistical uncertainty) of 1% per control point as per the departmental protocol was used on an Infinity® linear accelerator (Elekta, Stockholm, Sweden) with Agility® multi-leaf collimator (MLC). For the conventional 3DCRT plans parallel, opposed bilateral and a single posterior field were used as illustrated previously [3]. A feathering technique was used, where the length of the spinal PTV is more than 20 cm. IMRT and VMAT plans were created using the “bias dose” planning technique to achieve a uniform dose distribution at the junction. The planning technique followed for IMRT is described previously [27]. VMAT plans on the other hand had  $\pm 50^\circ$  arc from  $0^\circ$  or  $180^\circ$ . Tomotherapy plans were generated with a fan beam thickness of 2.5 cm, pitch of 0.3 and a modulation factor of three as described earlier with the Hi-ART treatment

system [27]. The optimization was continued until OAR doses could not be reduced any further without compromising coverage or increasing hot spots. For PBT planning IBA Proteus One machine model was used in RayStation. In Pencil beam scanning PBT plans, a vertebral-body-sparing technique was used as explained here [28] with a relative biological effectiveness (RBE) factor of 1.1. However, the difference in SMN risk between PBS with and without vertebral sparing is negligible. Dose wash comparison for all the techniques used in the study is shown in Fig. 1 for a representative patient. DVHs for some of the OARs included in the study is shown in Fig. 2.

## SMN risk modelling

Lifetime attributable risk (LAR) was chosen as the primary risk measure in this study as recommended by BEIR VII [25]. To calculate the LAR, dose-volume histograms of critical structures contoured were extracted for all the plans and converted to organ equivalent doses (OED) using the LNT and a mechanistic DRM as shown in Eq. 1. A detailed description of the mechanistic model can be found here [29]. Further, OED values were converted to excess absolute risk (EAR) to calculate LAR.

$$OED_i = \frac{1}{V_T} V_i RED_i \quad (1)$$

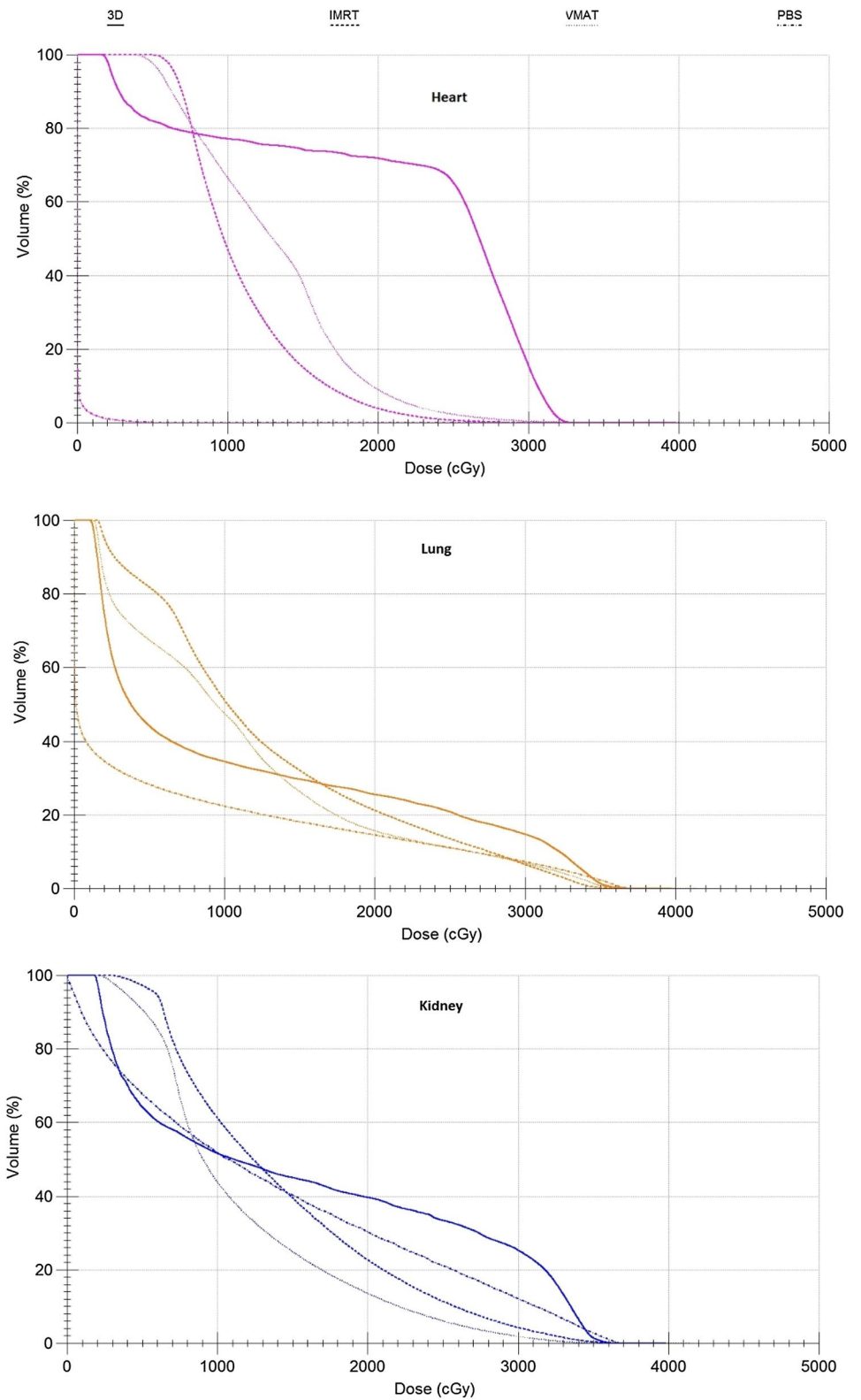
where  $V_T$  is the total volume of the organ of interest,  $V_i$  is the volume and  $RED_i$  is the risk-equivalent dose in the  $i_{th}$  DVH bin.  $RED$  is calculated as shown in Eqs. 2 and 3 for linear and mechanistic DRM.

$$RED_{linear} = D \quad (2)$$



**Fig. 1** Dose wash comparison of 3DCRT, IMRT, VMAT, HT and pencil beam scanning PBT. Color wash shown above 50% of the prescription dose (irradiated volume)

**Fig. 2** DVH comparison of some of the organs included in the study



$$RED_{mechanistic} = \frac{\exp(-\alpha'D)}{\alpha'R} (1 - 2R + R^2 \exp(\alpha'D) - (1 - R)^2 \exp\left(-\left(\frac{\alpha'R}{(1 - R)}\right)D\right)) \quad (3)$$

where  $\alpha'$  in the mechanistic DRM was calculated as shown in Eq. 4.

$$\alpha'_i \alpha + \beta d \quad (4)$$

where  $\alpha$  and  $\beta$  are the cell-kill parameters of the linear-quadratic model,  $D$  is the total dose and  $d$  is the dose per fraction.  $R$  is the repopulation parameter ranging from 0 for no repopulation to 1 for full repopulation. EAR was calculated according to Eq. 5.

$$EAR_{org} = \frac{1}{V_T} \sum_i V_i RED_i \beta' \mu(age_x, age_a) (1 \pm s) \quad (5)$$

where  $V_T$  is the total volume of the organ,  $V_i$  is the volume and  $RED_i$  is the risk-equivalent dose in the  $i$ th DVH bin.  $\beta'$  is the initial slope of the dose–response curve for radiation-induced second cancers and  $\mu$  is a modifying factor that accounts for patient’s age at exposure ( $age_x$ ) and age at which the risk is estimated ( $age_a$ ) which is calculated as shown in Eq. 6.

$$\mu(age_x, age_a) = \exp\left(\gamma_e (age_x - 30) + \gamma_a \left(\ln\left(\frac{age_a}{70}\right)\right)\right) \quad (6)$$

where  $\gamma_e$  and  $\gamma_a$  are age modifying factors and  $\beta'$  is originally defined for persons exposed at age 30 and attaining age of 70 years. The EAR was calculated by assuming  $age_x$  as 30 years and also with the actual patient’s age to demonstrate the impact of age into EAR calculation. The  $age_a$  is set to 70 years for all patients. An  $\alpha'$  value of  $0.018 \text{ Gy}^{-1}$

and a repopulation factor  $R$  of 0.93 was used in the mechanistic model for carcinoma induction [29]. Gender specific correction factor of 0.17 and  $-0.17$  for females and males were used for the EAR calculation as recommended in the literature [18]. LAR was calculated as shown in Eq. 7.

$$LAR = \int_{age_{x+L}}^{age_{a,0}} EAR(D, age_x, age_a) \frac{S(age_a)}{S(age_x)} d(age_a) \quad (7)$$

The integration over EAR was performed over an attained age from a latent period ( $L$ ) of solid cancer induction after the exposure ( $L = 5$  years) to  $age_a$  of 70 years. The ratio  $S(age_a)/S(age_x)$  defines the probability of surviving from age at exposure to the attained age, which was obtained from life table for the US population [30].

### Results

The mean dose averaged over all ten patients for various organs are shown in Fig. 3 with 95% confidence intervals calculated by the bootstrap method. The mean dose was substantially lesser in PBS plans compared to all other plans for organs that are farther to the target volumes such as esophagus, liver, heart, bowel and stomach. However, organs closer to the target volumes such as lungs and kidney had comparable mean dose to other organs in all plans. 3DCRT plans in general had highest mean doses due to larger volumes of normal tissue receiving dose around 50% of the prescribed dose. This can be corroborated with Figs. 1, 2 and 3. Relative mean integral dose was also calculated by averaging over all organs and by normalizing it to the average of all

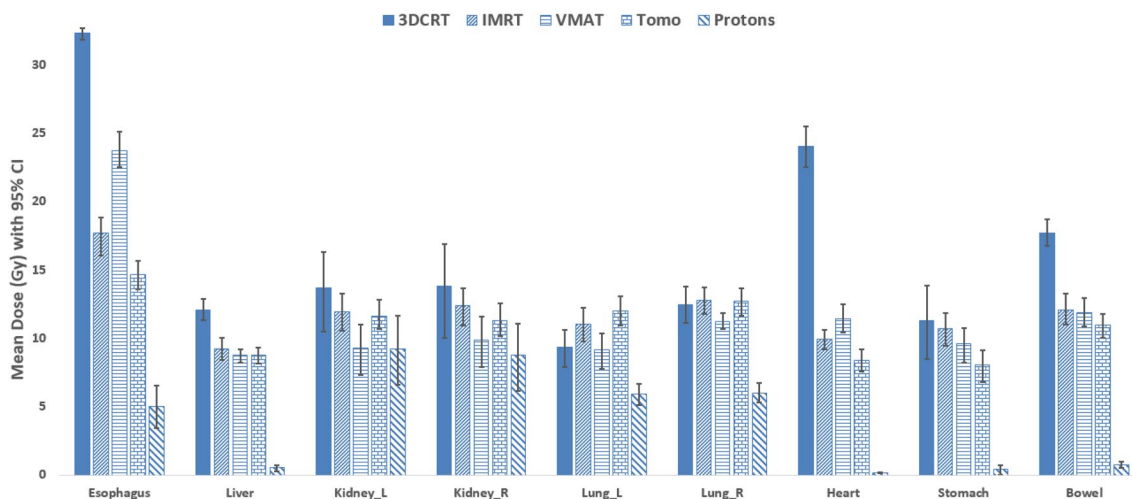


Fig. 3 Mean doses and 95% confidence intervals calculated for organs-at-risk for cranio-spinal irradiation treatment plans planned with 3DCRT, IMRT, VMAT, Tomotherapy and Proton beam therapy

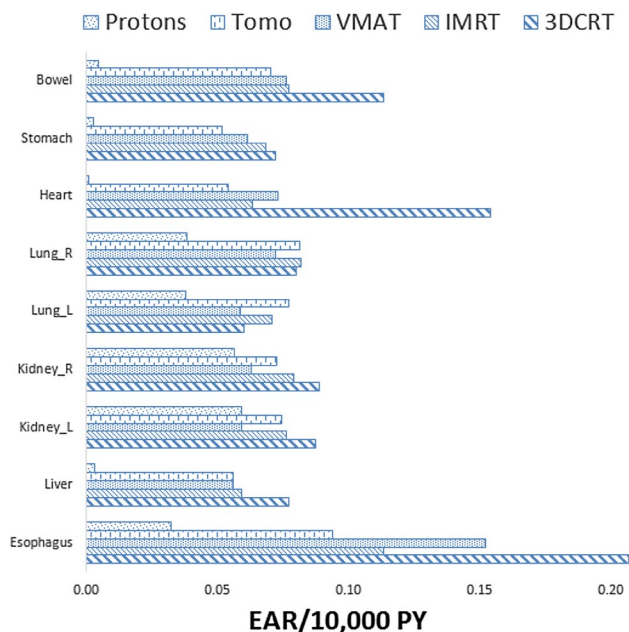


Fig. 4 Site-specific EAR with the linear dose–response model

organ mean dose in PBS plans. The relative mean integral dose was 6.3, 4.8, 4.5 and 4.7 times higher compared to PBS plans respectively in 3DCRT, IMRT, VMAT and HT plans. Site-specific EAR is shown in Fig. 4 with the linear dose–response model.

The organ average EAR (10,000 PY<sup>-1</sup>) with the linear model ranged from 0.07 to 0.10 for male and from 0.04 to 0.15 for female patients with X-ray-based plans, while it was 0.03 and 0.04 for male and female patients with PBS respectively. The mean EAR values are shown in Fig. 5 for the linear and mechanistic models. The EAR was slightly higher for the 3DCRT plans compared to other plans in

the linear model, however with the mechanistic model it is slightly lower compared to IMRT, VMAT and tomotherapy plans. All other plans except PBS had similar EAR for male and female patients in both linear and mechanistic models. The mean LAR showed a similar trend as EAR for both models as shown in Fig. 6. The relative risk (rLAR) [18] calculated as LAR/LAR<sub>PBS</sub> is shown in Fig. 7. The rLAR ranged from 1.0 to 4.0 for male and female patients with the linear model, whereas it was from 1.0 to 3.8 for male and female patients compared to PBS plans. The results are summarized in Table 1 for both linear and mechanistic models.

### Discussion

Our study showed that the relative lifetime risk of developing SMN after CSI was 2.7–4.0 times higher in X-ray-based techniques compared to PBS plans for both male and female patients respectively with the linear model. The same values were 2.2–3.8 times higher for male and female patients respectively with the mechanistic model. These values were within the range of 1.3–4.6 reported by Moteabbed et al. [18] for lifetime risk of SMN development in head and neck patients treated by IMRT/VMAT compared to PBS. The EAR was proportionately higher in all plans for female patients compared to males due to the gender-specific correction factor of 1.17 applied in calculating EAR for female patients for both linear and mechanistic models. This in turn reflected in higher mean LAR for female patients in all plans compared to male patients for both models.

The mean LAR for IMRT, VMAT and HT plans were almost similar, whereas 3DCRT plans had higher mean LAR than PBS in the linear model but lower compared to IMRT, VMAT and HT plans in the mechanistic model.

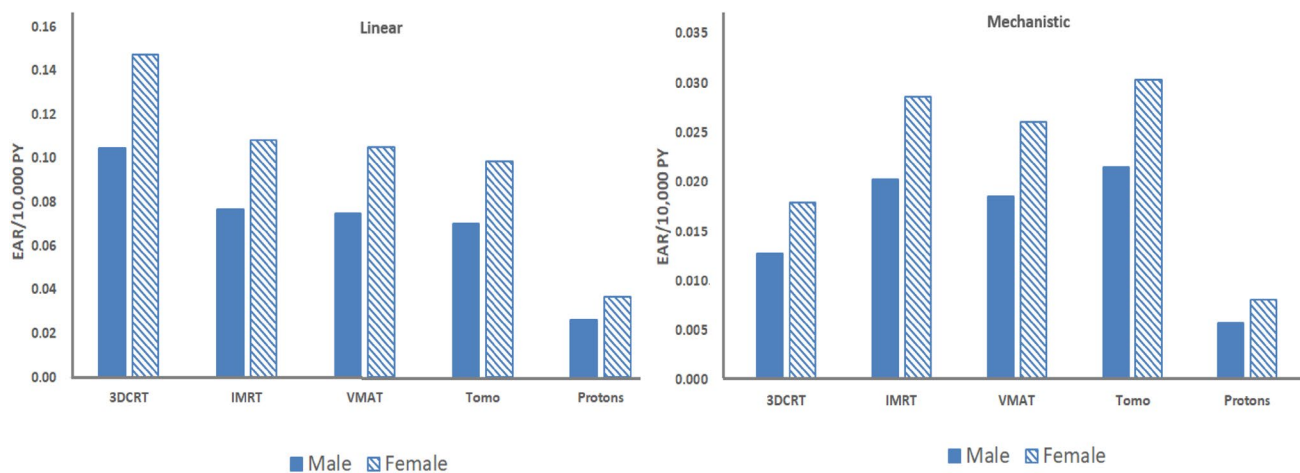


Fig. 5 Mean EAR for male and female patients for the linear and mechanistic model

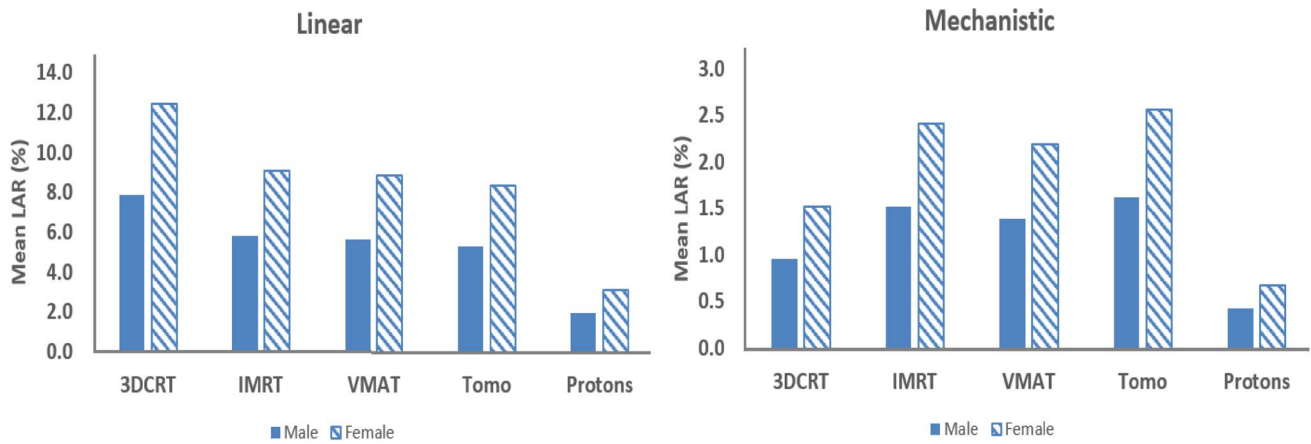


Fig. 6 The mean LAR for various techniques with the linear and the mechanistic model

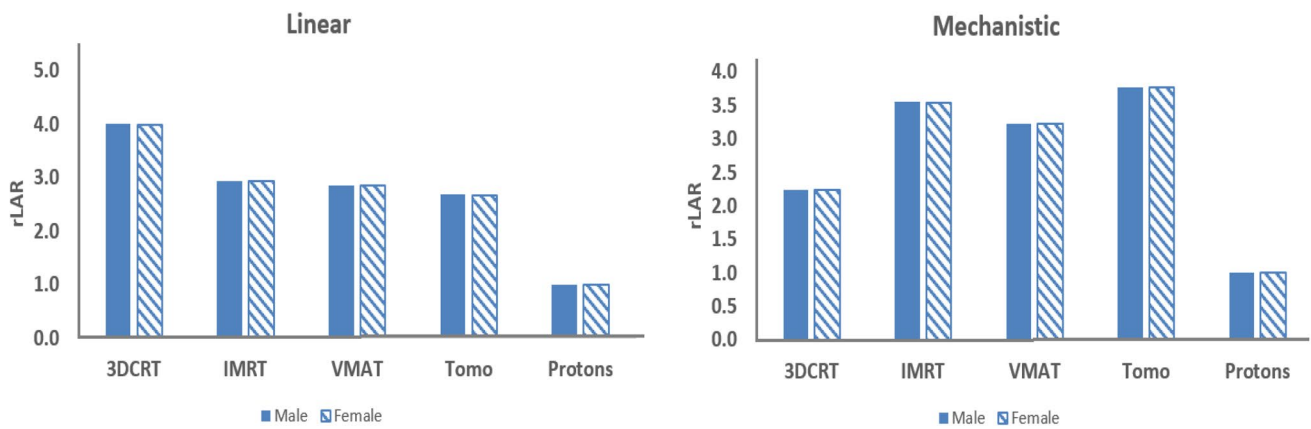


Fig. 7 Relative LAR (rLAR) for various techniques with the linear and the mechanistic model

**Table 1** Summary of the results for the linear dan mechanistic models for various organs used in the study

Technique	EAR <sub>male</sub> (10,000PY <sup>-1</sup> )	EAR <sub>female</sub> (10,000PY <sup>-1</sup> )	mean LAR <sub>male</sub> (%)	LAR <sub>female</sub> (%)	rLAR <sub>male</sub> (unitless)	rLAR <sub>female</sub> (unitless)
Linear model						
3DCRT	0.10	0.15	7.87	12.41	4.0	4.0
IMRT	0.08	0.11	5.78	9.10	2.9	2.9
VMAT	0.07	0.11	5.63	8.86	2.9	2.8
Tomo	0.07	0.10	5.28	8.32	2.7	2.7
Protons	0.03	0.04	1.97	3.11	1.0	1.0
Mechanistic model						
3DCRT	0.01	0.02	0.96	1.52	2.2	2.2
IMRT	0.02	0.03	1.53	2.41	3.6	3.5
VMAT	0.02	0.03	1.39	2.19	3.2	3.2
Tomo	0.02	0.03	1.62	2.56	3.8	3.8
Protons	0.01	0.01	0.43	0.68	1.0	1.0

This can be attributed to the dose–response function of the mechanistic model that reduces the risk at higher doses due to predominant cell kill in contrast to cell mutation

at low doses that are more likely to turn malignant [7, 21]. However, the risk is shown to be substantially lower in PBS plans compared to all other plans for both male

and female patients in the linear and mechanistic model. Exceptionally, 3DCRT plans had lower risk than other X-ray based plans and in the mechanistic model. This can also be attributed to the dose–response relation modeled by the mechanistic model, where higher doses are associated with lower risk; which is the case with 3DCRT. The rLAR in IMRT, VMAT and HT plans were similar to the findings of Mirabell et al. [31] where protons have been shown to reduce the risk (relative risk compared to standard X-ray plans) by a factor of 2.4. In contrast to this, Zhang et al. [15] reported a slightly higher reduction in protons compared to photons. i.e., photon to proton LAR ratio of 0.18 (5.5 times reduction in risk in protons) using a single medulloblastoma patient treated by CSI with a three-field photon and a four-field passive scattering plan. This increased reduction found by Zhang et al. was due to the fact that a passive scattering technique was used in their study which increases the risk due to the production of secondary neutrons by the scattering foils employed, which they also accounted for in the risk estimation. The comparable risk in IMRT and VMAT found in our study was also reported by Moteabbed et al. [18] in head and neck patients since even a few field IMRT will cover most of the relatively smaller organs in younger patients. This also makes the dependency of SMN risk on number of fields in IMRT negligible in younger patients.

Our study has provided a comprehensive comparison of lifetime risk in CSI with various treatment techniques using theoretical risk assessment methods based on realistic patient data. It should be noted that the parameters used in this study is based on a totally different; genetically more susceptible patient group [32]. This might lead to an overestimation of the absolute risk found in this study. However, relative values are arguably less affected by applying the same parameters using the same model for different treatment techniques. This justified the use of rLAR as a primary measure of comparing risk in different techniques. Another limitation is the negligence of neutron dose from the proton beam in our risk analysis. However, it was shown to be very low by Monte Carlo simulations, i.e., 0.4% of the risk [18]. Moreover, the rest of the X-ray-based techniques only employed 6MV which also has negligible neutron production. Hence, this should not affect the results found in this study significantly.

## Conclusions

The reduction in SMN risk was found to be two to three times and two to four times in PBS plans compared to X-ray based techniques in male and female patients respectively based on the commonly used linear model.

Tomotherapy had comparable risk to IMRT and VMAT, whereas 3DCRT had higher risk among all plans. The results were comparable with the mechanistic model except, a reduction in risk in 3DCRT compared to IMRT, VMAT and tomotherapy plans.

## Compliance with ethical standards

**Conflict of interest** The authors declare that they have no conflict of interest.

**Ethical approval** The ethics was approved by the local institutional ethics committee.

## References

1. Frühwald MC, Rutkowski S (2011) Tumors of the central nervous system in children and adolescents. *Dtsch Arztebl* 108(22):390–397
2. Slampa P, Pavelka Z, Dusek L, Hynkova L, Sterba J, Ondrova B, Princ D, Novotny T, Kostakova S (2007) Longterm treatment results of childhood medulloblastoma by craniospinal irradiation in supine position. *Neoplasma* 54(1):62–67
3. Athiyaman H, Mayilvaganan A, Singh D (2014) A simple planning technique of craniospinal irradiation in the eclipse treatment planning system. *J Med Phys* 39(4):251–258
4. Seppälä J, Kulmala J, Lindholm P, Minn H (2010) A method to improve target dose homogeneity of craniospinal irradiation using dynamic split field IMRT. *Radiother Oncol* 96(2):209–215
5. Peñagaricano J, Moros E, Corry P, Saylor R, Ratanatharathorn V (2009) Pediatric craniospinal axis irradiation with helical tomotherapy: patient outcome and lack of acute pulmonary toxicity. *Int J Radiation Oncol Biol Phys* 75:1155–1161
6. Kunos CA, Dobbins DC, Kulasekera R, Latimer B, Kinsella TJ (2008) Comparison of helical tomotherapy versus conventional radiation to deliver craniospinal radiation. *Technol Cancer Res Treat* 7(3):227–233
7. Hall EJ (2006) Intensity-modulated radiation therapy, protons, and the risk of second cancers. *Int J Radiat Oncol Biol Phys* 65:1–7
8. Lindell B et al (1990) International Commission on Radiological Protection. Recommendations. *Annals of the ICRP Publication* 60. Pergamon Press, Oxford
9. Friedman DL et al (2010) Subsequent neoplasms in 5-year survivors of childhood cancer: the childhood cancer survivor study. *J Natl Cancer Inst* 102:1083–1095
10. Hall EJ, Wu C (2003) Radiation-induced second cancers: the impact of 3D-CRT and IMRT. *Int J Radiat Oncol Biol Phys* 56:83–88
11. Smith MA et al (2010) Outcomes for children and adolescents with cancer: challenges for the twenty-first century. *J Clin Oncol* 28:2625–2634
12. Tubiana M (2009) Can we reduce the incidence of second primary malignancies occurring after radiotherapy? A critical review. *Radiother Oncol* 91:4–15
13. Yan X, Titt U, Koehler AM et al (2002) Measurement of neutron dose equivalent to proton therapy patients outside of the proton radiation field. *Nucl Instrum Method Phys Res A* 476:429–434

14. Newhauser WD, Durante M (2011) Assessing the risk of second malignancies after modern radiotherapy. *Nat Rev Cancer* 11(6):438
15. Zhang R et al (2013) Comparison of risk of radiogenic second cancer following photon and proton craniospinal irradiation for a pediatric medulloblastoma patient. *Phys Med Biol* 58(4):807–823
16. Schneider U, Antony L, Norbert L (2000) Comparative risk assessment of secondary cancer incidence after treatment of Hodgkin's disease with photon and proton radiation. *Radiat Res* 154(4):382–388
17. Grantzau T, Lene M, Jens O (2013) Second primary cancers after adjuvant radiotherapy in early breast cancer patients: a national population based study under the Danish Breast Cancer Cooperative Group (DBCG). *Radiother Oncol* 106(1):42–49
18. Moteabbed M, Yock TI, Paganetti H (2014) The risk of radiation-induced second cancers in the high to medium dose region: a comparison between passive and scanned proton therapy, IMRT and VMAT for pediatric patients with brain tumors. *Phys Med Biol* 59(12):2883
19. Jarlskog CZ, Harald P (2008) Risk of developing second cancer from neutron dose in proton therapy as function of field characteristics, organ, and patient age. *Int J Radiat Oncol Biol Phys* 72(1):228–235
20. Athar BS, Paganetti H (2011) Comparison of second cancer risk due to out-of-field doses from 6-MV IMRT and proton therapy based on 6 pediatric patient treatment plans. *Radiother Oncol* 98(1):87–92
21. Sakthivel V, Mani GK, Mani S, Boopathy R, Selvaraj J (2017) Estimating second malignancy risk in intensity-modulated radiotherapy and volumetric-modulated arc therapy using a mechanistic radiobiological model in radiotherapy for carcinoma of left breast. *J Med Phys* 42(4):234
22. Daşu A, Toma-Daşu I, Olofsson J, Karlsson M (2005) The use of risk estimation models for the induction of secondary cancers following radiotherapy. *Acta Oncol* 44(4):339–347
23. Kumar S (2012) Second malignant neoplasms following radiotherapy. *Int J Environ Res Public Health* 9(12):4744–4759
24. Armstrong GT, Sklar CA, Hudson MM, Robison LL (2007) Long-term health status among survivors of childhood cancer: does sex matter? *J Clin Oncol* 25(28):4477–4489
25. BEIR (2006) Health risks from exposure to low levels of ionizing radiation BEIR VII phase 2. National Research Council, National Academy of Science, Washington
26. Taddei PJ, Mahajan A, Mirkovic D, Zhang R, Giebeler A, Korn-guth D, Harvey M, Woo S, Newhauser WD (2010) Predicted risks of second malignant neoplasm incidence and mortality due to secondary neutrons in a girl and boy receiving proton craniospinal irradiation. *Phys Med Biol* 55(23):7067
27. Sharma DS, Gupta T, Jalali R, Master Z, Phurailatpam RD, Sarin R (2009) High-precision radiotherapy for craniospinal irradiation: evaluation of three-dimensional conformal radiotherapy, intensity-modulated radiation therapy and helical Tomo therapy. *Br J Radiol* 82(984):1000–1009
28. Brown AP, Barney CL, Grosshans DR, McAleer MF, De Groot JF, Puduvalli VK, Tucker SL, Crawford CN, Khan M, Khatua S, Gilbert MR (2013) Proton beam craniospinal irradiation reduces acute toxicity for adults with medulloblastoma. *Int J Radiat Oncol Biol Phys* 86(2):277–2784
29. Schneider U (2009) Mechanistic model of radiation-induced cancer after fractionated radiotherapy using the linear-quadratic formula. *Med Phys* 36(4):1138–1143
30. Anderson RN, DeTurk PB (2002) United States life tables 1999. *Natl Vital Stat Rep* 50:1–39
31. Miralbell R, Lomax A, Cella L, Schneider U (2002) Potential reduction of the incidence of radiation-induced second cancers by using proton beams in the treatment of pediatric tumors. *Int J Radiat Oncol Biol Phys* 54(3):824–829
32. Schneider U, Marcin S, Judith R (2011) Site-specific dose-response relationships for cancer induction from the combined Japanese A-bomb and Hodgkin cohorts for doses relevant to radiotherapy. *Theor Biol Med Model* 8(1):27

**Publisher's Note** Springer Nature remains neutral with regard to jurisdictional claims in published maps and institutional affiliations.